.

Forming-free high-endurance Al/ZnO/Al memristor fabricated by dual ion beam sputtering

Amitesh Kumar, Mangal Das, Vivek Garg, Brajendra S. Sengar, Myo Than Htay, Shailendra Kumar, Abhinav Kranti, and Shaibal Mukherjee

Citation: Appl. Phys. Lett. **110**, 253509 (2017); doi: 10.1063/1.4989802
View online: http://dx.doi.org/10.1063/1.4989802
View Table of Contents: http://aip.scitation.org/toc/apl/110/25
Published by the American Institute of Physics

AIP | Applied Physics Letters
Save your money for your research.
It's now FREE to publish with us -
no page, color or publication charges apply.
If your article has the potential to shape the future of applied physics, it BELONGS in Applied Physics Letters

CrossMark click for updates

Forming-free high-endurance Al/ZnO/Al memristor fabricated by dual ion beam sputtering

Amitesh Kumar,[1,2] Mangal Das,[1] Vivek Garg,[1] Brajendra S. Sengar,[1] Myo Than Htay,[3] Shailendra Kumar,[4] Abhinav Kranti,[2] and Shaibal Mukherjee[1,a)]

[1]*Hybrid Nanodevice Research Group (HNRG), Electrical Engineering, Indian Institute of Technology Indore, Simrol, Indore 453552, India*

[2]*Low Power Nanoelectronics Research Group, Electrical Engineering, Indian Institute of Technology Indore, Simrol, Indore 453552, India*

[3]*Hashimoto-Myo Laboratory, Department of Electrical and Computer Engineering, Shinshu University, 4-17-1 Wakasato, Nagano City, Nagano Prefecture, 380-8553 Japan*

[4]*Raja Ramanna Center for Advanced Technology, Indore-452013, India*

(Received 11 April 2017; accepted 7 June 2017; published online 22 June 2017)

We report dual ion beam sputtering fabrication of an Al/ZnO/Al memristor displaying forming-free bipolar resistive switching characteristics with memristive behavior without necessitating any post-processing steps. A nearly amorphous ZnO thin film and an appropriate concentration of oxygen vacancies play a significant role in imparting forming-free, stable, and reliable behavior to memory cells. Besides, sufficient non-lattice oxygen ions in the film play a crucial role in the resistive switching process. The AlO_x interface layer is observed to strongly affect the switching mechanism in the memory device by altering the barrier at the Al/ZnO interface. The device shows stable switching behavior for >250 cycles with good retention and stable set/reset voltages. *Published by AIP Publishing.*
[http://dx.doi.org/10.1063/1.4989802]

Memristors, the so-called fourth fundamental element,[1] have drawn extensive attention in recent years for their great potential as next-generation non-volatile memory (NVM).[2] Resistive random-access memory (RRAM) being one of the major applications of memristors is a promising candidate to replace conventional charge-based flash memory in future owing to its simple structure, fast switching, low power consumption and high stacking density.[3,4] In recent years, the resistive switching (RS) phenomenon has been observed with wide band gap metal oxides (such as TiO_x, NiO_x, and ZnO) containing regulated oxygen vacancies.[3] ZnO is often classified as an n-type semiconductor whose electrical properties are mainly governed by the presence of electrically active and stoichiometric native point defects, such as vacancies and interstitials.[5] Pre-existing oxygen vacancies and non-lattice oxygen ions in ZnO bulk play a dominant role in attributing forming-free RS.

Bipolar resistive switching (BRS) with forming-free memristive behavior is generally not consistent among general fabrication processes. In general, unipolar switching devices require a high-voltage forming process, which affects their stability and causes damage to electrodes.[6] Further fluctuation of parameters such as set-voltage (V_{set}), reset-voltage (V_{reset}), high resistance state (HRS), and low resistance state (LRS) with operation cycles and time is a common concern among NVMs. High endurance and retention are essential for a reliable and stable memory cell. Herein, we report fabrication of a stable BRS with memristive behavior of forming-free Al/ZnO/Al memory cells fabricated by a dual ion beam sputtering (DIBS) system. The fabrication of ZnO based RRAM by the DIBS system has not been reported to date. Therefore, the study of the switching characteristics of ZnO based RRAM fabricated by DIBS and the corresponding relation with electrical, elemental and structural properties is very significant.

The DIBS system is equipped with a *radio-frequency* (RF) deposition ion source and *direct-current coupled* (DC) assist ion source.[7] As compared to single ion beam deposition, the film stoichiometry is enhanced in DIBS by mixing oxygen into the working gas (Ar) in the assist ion source.[8] Other salient features of DIBS are mentioned elsewhere.[7] First, a 250 nm layer of insulating SiO_2 is deposited upon a thoroughly cleaned (in trichloroethylene, acetone and isopropanol and further purged by 99.999% pure nitrogen gas) commercially available *n*-type low resistive (1–5 Ω/cm) Si (100) substrate at room temperature (RT). Further, a 150 nm layer of Al is sputtered upon it as the bottom electrode. A 60 nm thick ZnO layer (switching layer) is deposited over the bottom Al electrode, using a sintered ZnO target (99.99%) at a substrate temperature of 100 °C. DIBS background pressure of 1×10^{-8} mBar, working pressure of 2×10^{-4} mBar, and ion beam power of 70 W are used. During ZnO growth, the discharge voltage and the current of the assist ion source are maintained at 60 V and 600 mA, respectively. The flow rates of O_2 and Ar are maintained at 3 and 2 sccm, respectively, in the deposition source. Finally, a circular Al top electrode with a diameter of 500 μm is patterned on the surface of ZnO using a metal shadow mask at room temperature in a pure Ar ambient atmosphere.

ZnO crystallinity has been analyzed by a Bruker D8 Advance X-ray diffractometer (XRD) (Cu Kα, $\lambda = 0.1541$ nm). To analyze the binding energy and the composition of each element in the ZnO switching layer, X-ray photoelectron spectroscopy (XPS), which has a PHOIBOS 100 analyzer with Al Kα radiation (1486.6 eV) as an excitation source, has been utilized.

a)Author to whom correspondence should be addressed: shaibal@iiti.ac.in. Telephone: +91-731-2438916.

Photoluminescence (PL) studies of the ZnO films have been carried out at room temperature by using a 20 mW continuous wave He-Cd laser having an excitation wavelength of 325 nm. The current-voltage (I-V) characteristics of the device are measured using a Keithley 2612 A sourcemeter and Everbeing probe-station. To verify the formation of any interfacial layer at the Al/ZnO interface, the sample has been studied by cross-sectional high-resolution transmission electron microscopy (HR-TEM) using a HR-TEM: JEOL JEM-2010.

The inset of Fig. 1(a) shows the schematic of our metal-insulator-metal device structure. Figure 1(a) shows the XRD pattern of thin film ZnO, which shows a nearly amorphous phase of ZnO. Owing to a low substrate temperature of 100 °C, mobility of the sputtered material reduces, leading to almost an amorphous form of the ZnO. Materials lacking grain boundaries would be desirable as a switching material in a memory cell, since it favors better mobility of the oxygen vacancies or the ions in the ZnO film.[6] Figure 1(b) shows XPS of the O 1s core level of ZnO. Before performing the measurement, the sample surface has been pre-sputtered using a 1 KeV Ar ion beam to remove the air contaminated top layer. The individual O 1s peak has been deconvoluted to generate the corresponding three distinct Lorentzian-Gaussian curves centered at binding energies 530.38 ± 0.15, 531.24 ± 0.15, and 532.42 ± 0.15 eV. The low binding energy curve at 530.38 ± 0.15 eV is attributed to O atoms at the regular lattice site (LO).[9] The medium binding energy curve at 531.24 ± 0.15 eV is attributed to the presence of O atoms in the oxygen deficient regions (VO) in ZnO.[9] Thus, oxygen vacancies are very likely to exist in the ZnO film. These defects play significant roles in the realization of a forming-free RS.[10,11] The highest binding energy curve at 532.42 ± 0.15 eV is attributed to the presence of interstitial O atoms (IO) or non-stoichiometric oxygen at the ZnO surface.[9,12] High content of non-lattice oxygen ions O^{2-} existing in ZnO assists recovery of oxygen vacancies during the reset process[13] and ensures stable switching characteristics. Figure 1(c) illustrates the XPS spectra of Zn 2p levels in ZnO. Zn $2p_{3/2}$ and Zn $2p_{1/2}$ levels have their peaks corresponding to binding energy at 1022.66 and 1045.72 eV, respectively, which are attributed to Zn atoms at regular lattice sites in ZnO bulk. The binding energy difference of 23.06 eV is in agreement with previously reported values of Zn^{2+} confirming the fully oxidized state of Zn atoms, i.e., Zn^{2+}. XPS spectra conform to the stoichiometric oxide layer of ZnO. This indicates the absence of any free metallic zinc ions, which negates probability of any metallic ion conduction. Further, VO and IO defects in ZnO have been investigated by PL measurement at room temperature, and the results are shown in Fig. 1(d). The sharp peak around 375 nm corresponds to the ZnO band gap (3.31 eV).[9] The origin of green emission (around 492 nm) is attributed to the presence of oxygen vacancy defects (VO) in ZnO crystals.[9] The broad orange luminescence around 625 nm results mainly owing to the presence of oxygen interstitials (IO) in ZnO.[9]

The typical RS of the device has been investigated by applying bias voltage to the top electrode (TE) while keeping the bottom electrode (BE) grounded. I-V characteristics obtained from the device are shown in Fig. 2(a). During the measurement, triangular voltage is swept in the sequence: $1 \rightarrow 2 \rightarrow 3 \rightarrow 4$, in the range of -7 and 7 V. The compliance current (CC) is restricted at 1 mA to prevent permanent breakdown of the device. While sweeping the voltage from 0 to -7 V, a sudden increase in current at -6.2 V (V_{set}) is observed as the device switches from HRS to LRS, said to be "set process." This LRS is maintained as voltage sweep is reversed from -7 to 0 V. However, on applying positive bias from 0 to 7 V, the device switches back from LRS to HRS at 6.3 V (V_{reset}), considered as "reset process." HRS is maintained as the bias is reversed from 7 back to 0 V. In succeeding I-V cycles, after completion of the first switching cycle, the device switches from LRS to HRS and back from HRS to LRS at nearly consistent set and reset voltages. This suggests that the DIBS fabricated device is forming-free and shows BRS with sharp set and reset voltage. Generally employed,

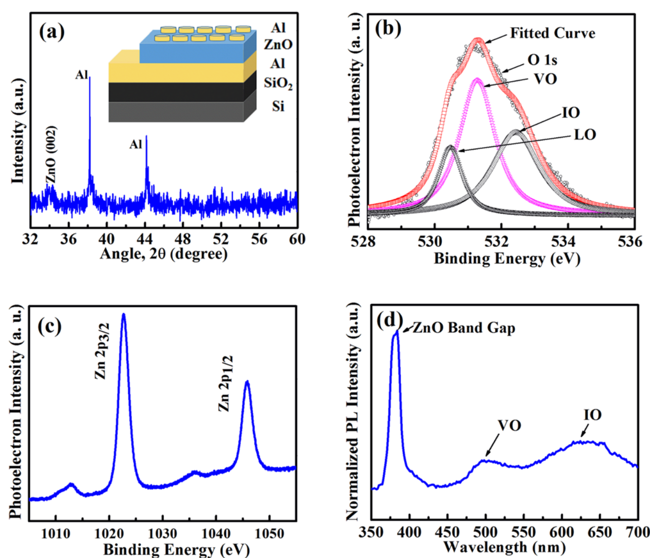

FIG. 1. (a) XRD of the ZnO film with the inset showing the device schematic, (b) XPS of O 1s spectra of thin film ZnO, (c) XPS spectra of Zn 2p levels in thin film ZnO, and (d) room temperature PL spectra of the ZnO film.

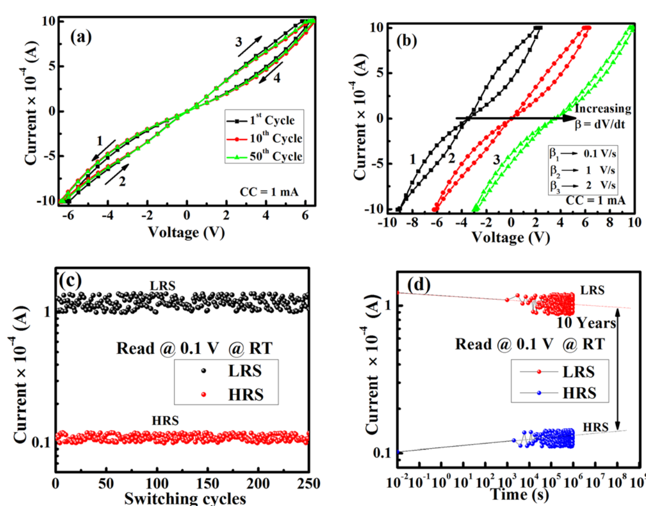

FIG. 2. (a) I-V characteristics in multiple cycles for CC of 1 mA, (b) I-V characteristics with increasing voltage sweep rate with hysteresis curves 1 and 3 shifted by 3.5 and -3.5 X-axis units, respectively, (c) Endurance tests of 250 cycles for homogeneous resistive switching at a read bias of 0.1 V, and (d) Retention behavior within the 10^6 s at a read bias of 0.1 V.

a high voltage forming process[10,14] is not required in our pristine device to make it conducting due to abundant oxygen vacancies pre-existing in the ZnO film.[13] A forming-free cell as compared to a forming-necessary cell shows more stable RS characteristics and also avoids destruction of electrodes.[6] The investigated device also shows good reversibility and stability of the switching response, and continuously switches between its on (LRS) and off (HRS) states for 50 cycles [Fig. 2(a)]. Further, a voltage sweep rate is varied keeping CC constant at 1 mA to investigate the corresponding behavior as shown in Fig. 2(b). The I-V hysteresis loop is observed to be dependent on the bias sweep rate; and it shrinks to a smaller loop for higher sweep rates, conforming to memristive behavior.[15–17]

As we can observe from Fig. 2(c), HRS and LRS are shown as a function of the number of switching cycles measured at a reading voltage of 0.1 V at RT for our Al/ZnO/Al memory cell. As observed from the figure, the variation of HRS and LRS during cycling is consistent without much degradation. The HRS and LRS conduction mechanism differs owing to formation of an AlO_x layer. Lower Gibbs' free energy for formation of AlO_x to ZnO is responsible for device switching from LRS to HRS.[18] This interfacial behavior is not smooth upon consecutive voltage pulse application. Hence, differently distributed behavior is noticed for HRS and LRS.[19] The above endurance measurements ensured that the RS properties in Al/ZnO/Al devices are highly reliable and reproducible. Further, the RS retention characteristic is investigated as shown in Fig. 2(d). The resistances for both HRS and LRS states are demonstrated using a small reading voltage of 0.1 V, to confirm the non-volatility of resistance states. No significant switching degradation after the duration 1×10^6 s (11 days) by extrapolation is expected to prolong to 10 years with non-destructive readout.[20,21]

In general, reactive metal-ZnO interfaces are found to generate extrinsic defects due to reactions and/or inter-diffusions against non-reactive interfaces. Oxides of reactive metals such as Al and Ti have far lower standard Gibbs free energy for formation as compared to ZnO and oxides of inert electrodes (Pt and Au).[18] Moreover, strong affinity of Al for oxygen ions also increases oxygen vacancies near the interface assisting the formation of forming-free memory cells.[15] Figure 3(a) shows the HR-TEM image of the Al/ZnO interface of the device in HRS. It is observed that an amorphous AlO_x interfacial layer of approximately 4–5 nm is formed at the interface. The AlO_x interface layer strongly affects the switching mechanism in our device by altering the barrier at the Al/ZnO interface under the applied electric field.[22] In addition, the use of Al electrodes owing to the AlO_x layer improves device endurance.[23]

Figure 3(b) illustrates schematics of the Al/ZnO/Al memory cell in HRS and LRS states, depicting the roles of oxygen vacancies, oxygen ions, and AlO_x interfacial layer. Al is expected to form an ohmic contact with ZnO.[24] However, stoichiometric modulation of the oxygen-rich region at the interface of Al/ZnO introduces an asymmetric Schottky barrier height suppressing current in a voltage range limited to the difference of barrier heights.[5] In Fig. 3(b), as we apply a negative bias voltage, the positively charged oxygen vacancies would effectively migrate towards TE from the bulk[25] and oxygen ions (O^{2-}) migrate to Al(BE)/ZnO interface causing local oxidation, leading to an AlO_x barrier layer, which results in the lower current density and device moves into HRS.[18] During the set process as shown in Fig. 3(b), as negative bias decreases to zero and further positive voltage increases on the top Al electrode, O^{2-}s move away from the Al(BE)/ZnO interface and positively charged oxygen vacancies (VO) migrate towards the bottom Al electrode, leading to dissolution of the AlO_x barrier layer. Therefore, the current

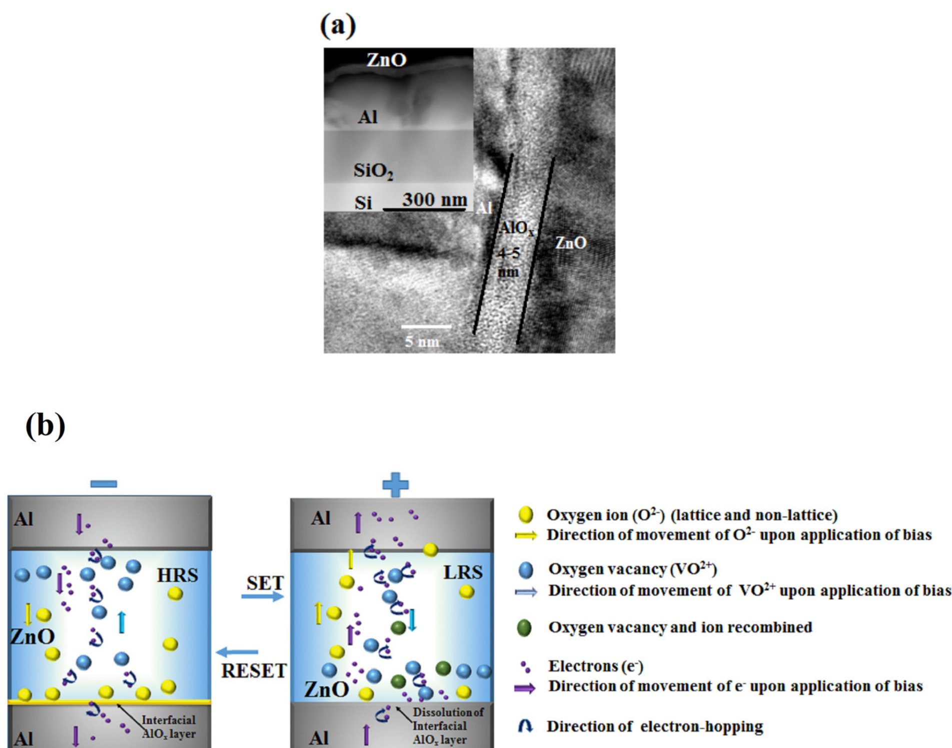

FIG. 3. (a) A clear interface layer of (~4–5 nm) is observed at the Al/ZnO interface of the device in the HRS state. The inset shows the Z-Contrast image of the cross-section of the device, (b) Switching mechanism of the device illustrating the SET process and RESET process.

TABLE I. Comparative analysis of different methods for RS device fabrication and corresponding device parameters. RT: Room Temperature *No sharp V_{set} and V_{reset} **Thicker memristive layer ***Post-processing (hydrogen surface annealing) is required.

Deposition technique	Device	ZnO thickness (nm)	Deposition temperature (°C)	Unipolar (Uni)/ Bipolar (Bi)	Forming	Set/reset voltage (V)	Retention (s)/endurance (cycles)	Reference
RF magnetron sputtering	Pt/ZnO/Pt	100	RT	Uni	Yes, 3.3 V	−2/−1	….	28
DC magnetron sputtering 1.5–3.2	Al/ZnO/Si	60	RT	Bi	No*	−7.8 to −3.2	…	18
Reactive sputtering	TiN/ZnO/Pt	30	450	Bi	Yes	1.2/−1.4	10^4/∼	13
DC reactive sputtering	Al/ZnO/Al	300	RT	Bi	No**	2/−2	∼/100	30
MOCVD	ITO/ZnO/ITO	100	200	Uni	Yes, 3.2 V	2.6/1.8	10^5/100	27
ALD	AZO/ZnO/Al	46–50	220	Bi	Yes, 13 V	10/−11	…	5
CBD	Pt/ZnO/Pt	100	95	Bi	Yes, 3.4 V	1.5/0.6	10^4/90	2
Hydrothermal	Au/ZnO/AZO	800	RT	Bi	No***	6/−6	∼/100	3
Electrodeposition	Ag/ZnO/Pt	350	RT	Bi	Yes	1/−1	∼/30	26
DIBS	Al/ZnO/Al	60	100	Bi	No	−6.2/6.3	(10^6/250)	Our work

density abruptly increases and the device sets to LRS. Similarly, by symmetry, the above mentioned mechanism is applicable to the Al(TE)/ZnO interface during positive bias with formation of an interfacial AlO_x layer [similar to Fig. 3(a)] to switch into positive-biased HRS. The generation/recovery of oxygen vacancies and oxygen ions during the set/reset has a significant role.[13] Sufficient non-lattice oxygen ions favor recovery as well as assist in the redox reaction at the Al/ZnO interface.[13] Besides, hopping of electrons through conducting paths of oxygen vacancies is assumed to be governing conduction in bulk.[13] Hence, the underlying RS mechanism is supposed to be a combination of electron hopping through conduction paths in bulk and redox reactions leading to formation and dissolution of the AlO_x layer at the interface.[22]

Table I provides an overview of different deposition techniques deployed to fabricate a resistive memory cell with ZnO as a switching material. DIBS as compared to atomic layer deposition (ALD)[5] is fast and does not require ultra-pure volatile precursors featuring a complex and time consuming process of fabrication. Further, DIBS as compared to many chemical deposition methods[2,3,26] gives more uniform and controlled deposition. The amount of oxygen vacancies and ions in different regions of the film can be controlled via modifying oxygen partial pressure during the ZnO growth. Low deposition temperature growth via DIBS ensures stable device performance as compared to other methods involving high deposition temperature.[5,13,27] Generally, usage of Pt electrodes in RRAM primarily shows a unipolar RS (URS) with ZnO,[28,29] and suffers from switching degradation[23] and deformation of the junction[14] due to oxygen bubble formation at metal/semiconductor contact. Al is economical as compared to Pt, promotes high endurance, and shows mostly BRS with ZnO.[18] Sun *et al.* have reported forming-free ZnO based memory cells with post-processing, i.e., hydrogen surface annealing.[3] Forming-free ZnO based memory cells as reported by Gul and Efeoglu have a larger thickness as compared to our device.[30] A lower thickness is preferable for RRAM cells.[3,31] The values of V_{set} and V_{reset} of the forming-free[18] memory cell reported by Chen *et al.* are not stable. However, in our case we have attained a stable set and reset voltage for device cut-off from forming-free memory cells.

In conclusion, an Al/ZnO/Al based memory cell having stable and reproducible BRS has been fabricated by DIBS. The device shows precise set/reset voltage (±∼6 V) and an excellent retention time (10^6 s) with an endurance test for more than 250 set/reset cycles. Forming-free behavior of the ZnO film is related to the deposition process and the resultant internal microstructure. The amorphous-like ZnO film having an appropriate amount of oxygen vacancies and non-lattice oxygen ions is attributed to the forming-free, BRS behavior with stable V_{set} and V_{reset}. The stability and reliability of our device are high owing to memory cells being forming-free with enhanced endurance due to the interfacial AlO_x layer. Our work could play a crucial role in the realization of highly reliable memristive devices in the future.

The authors are thankful to DIBS, XRD, and PL facilities, which are an integral part of Sophisticated Instrument Centre (SIC) of IIT Indore, HR-TEM facility at Shinshu University Japan, and AIPES beamline Indus facility at RRCAT, Indore. We are thankful to Mr. Tomohiko Yamakami of Technical Division, Faculty of Engineering, Shinshu University for TEM imaging. Amitesh Kumar and Brajendra S. Sengar would like to thank Council of Scientific & Industrial Research (CSIR) for providing fellowship. Mangal Das would like to thank DeiTY, Ministry of Electronics and Information Technology, Government of India, for providing fellowship under Visvesvaraya PhD Scheme for Electronics and Information Technology. Vivek Garg would like to thank University Grants Commission (UGC) for providing fellowship. Prof Shaibal Mukherjee is thankful to DeiTY, Ministry of Electronics and Information Technology, Government of India for the Young Faculty Research Fellowship (YFRF) under the Visvesvaraya PhD Scheme for Electronics and Information Technology.

[1] L. O. Chua, IEEE Trans. Circuit Theory **18**, 507 (1971).
[2] C. H. Huang, J. S. Huang, S. M. Lin, W. Y. Chang, J. H. He, and Y. L. Chueh, ACS Nano **6**, 8407 (2012).
[3] Y. Sun, X. Yan, X. Zheng, Y. Liu, Y. Zhao, Y. Shen, Q. Liao, and Y. Zhang, ACS Appl. Mater. Interfaces **7**, 7382 (2015).
[4] D. Liu, N. Wang, G. Wang, Z. Shao, X. Zhu, C. Zhang, and H. Cheng, Appl. Phys. Lett. **102**, 134105 (2013).
[5] R. Mundle, C. Carvajal, and A. K. Pradhan, Langmuir **32**, 4983 (2016).

[6]Y. Huang, Z. Shen, Y. Wu, X. Wang, S. Zhang, X. Shi, and H. Zeng, RSC Adv. **6**, 17867 (2016).
[7]R. Singh, P. Sharma, M. A. Khan, V. Garg, V. Awasthi, A. Kranti, and S. Mukherjee, J. Phys. D: Appl. Phys. **49**, 445303 (2016).
[8]S. G. Yoon, Y. T. Kim, H. K. Kim, M. J. Kim, H. M. Lee, and D. H. Yoon, Mater. Sci. Eng. B **118**, 234 (2005).
[9]S. K. Pandey, S. K. Pandey, C. Mukherjee, P. Mishra, M. Gupta, S. R. Barman, S. W. D'Souza, and S. Mukherjee, J. Mater. Sci. Mater. Electron. **24**, 2541 (2013).
[10]Q. Mao, Z. Ji, and J. Xi, J. Phys. D: Appl. Phys. **43**, 395104 (2010).
[11]D. Lee and T. Tseng, J. Appl. Phys. **110**, 114117 (2011).
[12]A. Kim, K. Song, Y. Kim, and J. Moon, ACS Appl. Mater. Interfaces **3**, 4525 (2011).
[13]N. Xu, L. Liu, X. Sun, X. Liu, D. Han, Y. Wang, R. Han, J. Kang, and B. Yu, Appl. Phys. Lett. **92**, 232112 (2008).
[14]J. Joshua Yang, F. Miao, M. D. Pickett, D. A. A. Ohlberg, D. R. Stewart, C. N. Lau, and R. S. Williams, Nanotechnology **20**, 215201 (2009).
[15]J. Wang, B. Sun, F. Gao, and N. C. Greenham, Phys. Status Solidi Appl. Mater. Sci. **207**, 484 (2010).
[16]L. Chua and S. M. Kang, Proc. IEEE **64**, 209 (1976).
[17]L. Chua, Appl. Phys. A: Mater. Sci. Process. **102**, 765 (2011).
[18]C. Chen, F. Pan, Z. S. Wang, J. Yang, and F. Zeng, J. Appl. Phys. **111**, 13702 (2012).
[19]K. Chiang, J. Chen, and J. Wu, ACS Appl. Mater. Interfaces **4**, 4237 (2012).
[20]J. Qi, J. Huang, D. Paul, J. Ren, S. Chu, and J. Liu, Nanoscale **5**, 2651 (2013).
[21]H. Bae, B.-H. Lee, D. Lee, M.-L. Seol, D. Kim, J.-W. Han, C.-K. Kim, S.-B. Jeon, D. Ahn, S.-J. Park, J.-Y. Park, and Y.-K. Choi, Sci. Rep. **6**, 38324 (2016).
[22]J. S. Rajachidambaram, S. Murali, J. F. Conley, S. L. Golledge, and G. S. Herman, J. Vac. Sci. Technol., B: Microelectron. Nanometer Struct.—Process., Meas., Phenom. **31**, 01A104 (2013).
[23]H. Lv, M. Wang, H. Wan, Y. Song, W. Luo, P. Zhou, T. Tang, Y. Lin, R. Huang, S. Song, J. G. Wu, H. M. Wu, and M. H. Chi, Appl. Phys. Lett. **94**, 213502 (2009).
[24]L. J. Brillson and Y. Lu, J. Appl. Phys. **109**, 121301 (2011).
[25]J. Qiu, A. Shih, W. Zhou, Z. Mi, and I. Shih, J. Appl. Phys. **110**, 14513 (2011).
[26]A. S. Zoolfakar, R. Ab Kadir, R. A. Rani, S. Balendhran, X. Liu, E. Kats, S. K. Bhargava, M. Bhaskaran, S. Sriram, S. Zhuiykov, A. P. O'Mullane, and K. Kalantar-Zadeh, Phys. Chem. Chem. Phys. **15**, 10376 (2013).
[27]J. W. Seo, J. W. Park, K. S. Lim, J. H. Yang, and S. J. Kang, Appl. Phys. Lett. **93**, 223505 (2008).
[28]W.-Y. Chang, Y.-C. Lai, T.-B. Wu, S.-F. Wang, F. Chen, and M.-J. Tsai, Appl. Phys. Lett. **92**, 22110 (2008).
[29]Z. J. Liu, J. C. Chou, S. Y. Wei, J. Y. Gan, and T. R. Yew, IEEE Electron Device Lett. **32**, 1728 (2011).
[30]F. Gul and H. Efeoglu, Superlattices Microstruct. **101**, 172 (2017).
[31]D. B. Strukov, G. S. Snider, D. R. Stewart, and R. S. Williams, Nature **453**, 80 (2008).

Forming-free high-endurance Al / ZnO / Al memristor fabricated by dual ion beam sputtering

Kumar, Amitesh; Das, Mangal; Garg, Vivek; Sengar, Brajendra S; Htay, Myo Than; Kumar, Shailendra; Kranti, Abhinav; Mukherjee, Shaibal

01 amitesh kumar Page 3

30/8/2019 5:42

02 amitesh kumar Page 3

30/8/2019 5:42